Mechanical Buckling of Circular Orthotropic Bilayer Nanoplate Embedded in an Elastic Matrix under Radial Compressive Loading

Mohammad Ahmadpour
Department of Mechanical Engineering,
Mashhad branch, Islamic Azad University, Mashhad, Iran
E-mail: mohammadahmadpoor99@yahoo.com

Mohammad Esmail Golmakani *
Department of Mechanical Engineering,
Mashhad branch, Islamic Azad University, Mashhad, Iran
E-mail: m.e.golmakani@mshdiau.ac.ir
*Corresponding author

Mohammad Naser Sadraee Far
Department of Mechanical Engineering,
Ferdowsi University of Mashhad, Mashhad, Iran
E-mail: sadrayifar_m@yahoo.com

Received: 29 February 2020, Revised: 17 April 2020, Accepted: 19 April 2020

Abstract: This article investigates the buckling behavior of orthotropic annular/circular bilayer graphene sheet embedded in Winkler–Pasternak elastic medium under mechanical loading. Using the nonlocal elasticity theory, the bilayer graphene sheet is modeled as a nonlocal orthotropic plate which contains small scale effect and van der Waals interaction forces. Differential Quadrature Method (DQM) is employed to solve the governing equations for various combinations of simply supported or clamped boundary conditions. The results show that small scale parameter does not have any effect on critical buckling load of cases without elastic medium in simply supported boundary condition. Also, increase of vdW coefficient leads to increase of critical buckling load smoothly then it has no impact on critical buckling load after a certain value.

Keywords: DQM, Mechanical Buckling, Nonlocal Mindlin Theory, Orthotropic Nanoplate

Reference: Mohammad Ahmadpour, Mohammad Esmail Golmakani, and Mohammad Naser Sadraee Far, "Mechanical Buckling of Circular Orthotropic Bilayer Nanoplate Embedded in an Elastic Matrix Under Radial Compressive Loading", Int J of Advanced Design and Manufacturing Technology, Vol. 14/No. 1, 2021, pp. 101–113. DOI: 10.30495/admt.2021.1894490.1176

Biographical notes: Mohammad Ahmadpour is currently MSc student in Mechanical Engineering at Islamic Azad University of Mashhad, Iran. His research interests are Nanomechanics, Computational and Solid Mechanics. **Mohammad Esmail Golmakani** received his PhD, MSc and BSc degrees in Mechanical Engineering from Ferdowsi University of Mashhad, Iran. He is currently Associate Professor in Mechanical Engineering at Islamic Azad University of Mashhad, Iran. His current research interest includes Mechanics of Advanced Materials, Nanomechanics and Elasticity. **Mohammad Naser Sadraee Far** is currently PhD student in Mechanical Engineering at Ferdowsi University of Mashhad, Iran. His current research focuses on Nanomechanics, Computational Mechanics and Composites Structures.

1 INTRODUCTION

In recent years, nanoplates such as Graphene Sheets (GSs) have received huge attention from the researcher community for their superior properties and practical applications in many fields such as superfast microelectronics, micro- or nano-electromechanical systems (MEMS or NEMS), biomedical, bioelectrical, and nanocomposites [1–5]. Single Layered Graphene Sheets (SLGSs) are defined as a flat one-atom-thick carbon tightly packed into a two-dimensional honeycomb lattice. Since the mechanical behavior of SLGSs plays a major role in their potential applications, the mechanical analysis of nanoplates has become a subject of primary interest in recent studies [6].

The traditional continuum theory is considered as a scale free theory and thus lacks validity to anticipate the mechanical behaviors of nanostructures properly [7]. Recently, size-dependent continuum modeling of nanostructures has become popular among the scientific community because controlled experiments on nanoscale are difficult to implement and molecular dynamic simulations are highly computationally expensive and are not suitable for analyzing large scale systems. A variety of size-dependent continuum theories have been so far introduced such as couple stress theory [8], strain gradient elasticity theory [9-11] modified couple stress theory [12-14] and nonlocal elasticity theory [15–18] among which the nonlocal elasticity theory has been the most widely applied one [19–26].

Based on this theory, a lot of studies have so far examined buckling and vibration behaviors of SLGSs as well as their properties [27–42]. Civalek [43] studied elastic buckling behavior of skew shaped single-layer graphene sheets. He found that the critical buckling loads predicted by pure shear loading are always bigger than those predicted by the other loadings. The effect of the aspect ratio on buckling loads grows significantly for small skew angles of the skew graphene. Zenkour and Sobhy [44] investigated nonlocal elasticity theory for thermal buckling of nanoplates lying on Winkler–Pasternak elastic substrate medium. Their findings showed that the nanoplate with a small side-to-thickness ratio faces a large critical buckling temperature rise and the buckling temperature rise of a clamped-free plate is much greater than that of a plate under other boundary conditions.

Ansari and Sahmani [45] investigated prediction of biaxial buckling behavior of single-layered graphene sheets based on nonlocal plate models and molecular dynamics simulations. They reported that as opposed to the chirality which is trivial in the biaxial response of SLGSs, the varieties of types of nonlocal plate model make a relatively significant difference between the proposed appropriate values of nonlocal parameter corresponding to each one. Farajpour et al. [46] studied surface and nonlocal effects on the axisymmetric buckling of circular graphene sheets in thermal environment. Radebe and Adali [47] investigated buckling and sensitivity analysis of nonlocal orthotropic nanoplates with uncertain material properties. They found the most conservative buckling load given the bound on the uncertainties.

Ansari et al. [48] studied on the bending and buckling behaviors of Mindlin nanoplates considering surface energies. They showed that when the nanoplate is under biaxial loading, the critical buckling load corresponding to the lower modes is more sensitive to the surface energies. Anjomshoa et al. [49] investigated finite element buckling analysis of multi-layered graphene sheets on elastic substrate based on nonlocal elasticity theory. Mohammadi et al. [50] studied shear buckling of orthotropic rectangular graphene sheet embedded in an elastic medium in thermal environment. They found that unlike the low or room temperature, where the critical shear buckling load with thermal effect is larger than the critical shear buckling load without thermal effects, thermal load ratio is smaller than unity at high temperature environment.

Radic et al. [51] investigated buckling analysis of double-orthotropic nanoplates embedded in Pasternak elastic medium using nonlocal elasticity theory. They found that nonlocal effect imposes a stronger influence on higher buckling modes. Sarrami and Azhari [52] conducted a study on the use of bubble complex finite strip method in the nonlocal buckling and vibration analysis of single-layered grapheme sheets. They showed that the nanoplate is more sensitive to the nonlocal effects in the case of shear loading rather than compressive loading. Sarrami and Azhari [53] studied nonlocal vibration and buckling analysis of single and multi-layered graphene sheets using finite strip method including van der Waals effects. They found that nonlocal parameter effect is more prominent in the sheets which are more stiffened due to the partly tension loading or because of more rigid end conditions. Murmu et al. [54] studied nonlocal buckling of double-nanoplate-systems under biaxial compression. They concluded that increase of stiffness parameter brings uniaxial and biaxial buckling phenomenon closer while increase of aspect ratio widens uniaxial and biaxial buckling phenomenon. Farajpour et al. [55] investigated buckling of orthotropic micro/nanoscale plates under linearly varying in-plane load via nonlocal continuum mechanics. They showed that in the case of pure in-plane bending, the nonlocal effects are relatively more than other cases. Farajpour et al. [56] studied axisymmetric buckling of the circular graphene sheets with the nonlocal continuum plate model. They indicated that the difference between the two boundary conditions in non-dimensional buckling load decreases with increasing nonlocal parameter.

A review of literature shows that no literature has been taken into account the behaviour of circular bilayer graphene sheet embedded in an elastic matrix considering the effect of small scale parameter based on nonlocal continuum mechanics. This motivates us to investigate this problem here. So in order to fill this gap, the present paper is conducted to investigate the mechanical buckling analysis of circular bilayer graphene sheet with clamped and simply supported boundary condition using nonlocal continuum mechanics and the differential quadrature method. Using the principle of virtual work, the nanoplate equilibrium equations are derived in terms of the generalized displacements based on FSDT using the nonlocal differential constitutive relations of Eringen and the von Karman nonlinear strains. To verify the present results and formulations, some comparison studies are carried out between the obtained results and the available solutions in the literature. Excellent agreement between the obtained and available results is observed. Finally, the small scale effects on the buckling behavior of nanoplates are investigated by considering various parameters such as small scale parameter, boundary conditions, Winkler and Pasternak elastic foundations, aspect ratio.

2 GOVERNING EQUATIONS

The SLGS is modeled as a circular nanoplate and the elastic medium is defined by a two-parameter Pasternak elastic foundation. The geometry of a radially circular graphene plate with thickness h, radius r, under buckling load N is shown in "Fig. 1". According to the first-order shear deformation theory, the displacement field can be expressed as follows:

$$\begin{aligned} u(r,z) &= u_0(r) + z\,\phi(r) \\ v(r,z) &= 0 \\ w(r) &= w_0(r) \end{aligned} \tag{1}$$

Where u and w are the displacement components of the midplane along the r and z directions, respectively. Also, ϕ denotes the rotational function of the transverse normal about the z axis. The linear ∂^0 and nonlinear ∂^1 Von-Karman strain fields are as follows:

$$\begin{aligned} \varepsilon_r &= \overset{0}{\varepsilon}_r + z\ \overset{1}{\varepsilon}_r \\ \varepsilon_\theta &= \overset{0}{\varepsilon}_\theta + z\ \overset{1}{\varepsilon}_\theta \\ \gamma_{rz} &= \overset{0}{\gamma}_{rz} \end{aligned} \tag{2}$$

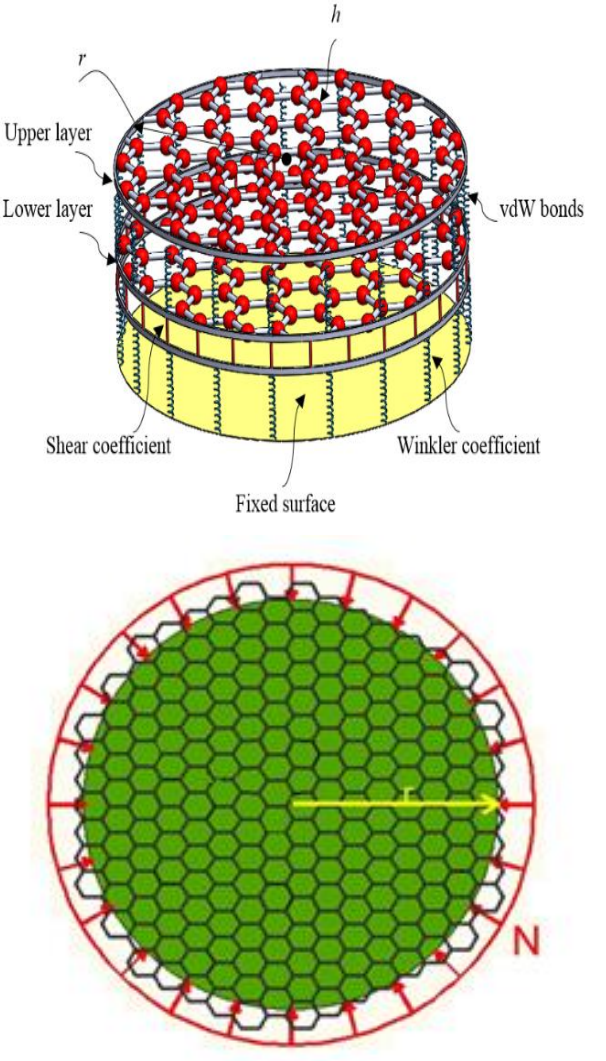

Fig. 1 The circular and annular bilayer graphene sheets in an atomic figure bridged on an elastic foundation.

In which:

$$\begin{aligned} \overset{0}{\varepsilon}_r &= \frac{\partial u_0}{\partial r} + \frac{1}{2}\left(\frac{\partial w_0}{\partial r}\right)^2 \\ \overset{1}{\varepsilon}_r &= \frac{\partial \phi}{\partial r} \\ \overset{0}{\varepsilon}_\theta &= \frac{u_0}{r} \\ \overset{1}{\varepsilon}_\theta &= \frac{1}{r}\phi \\ \overset{0}{\gamma}_{rz} &= \frac{\partial w_0}{\partial r} + \phi \end{aligned} \tag{3}$$

By substituting "Eq. (3)" into "Eq. (2)", the Von-Karman strain fields used can be expressed as:

$$\varepsilon_r = \frac{du_0}{dr} + z\frac{d\phi}{dr} + \frac{1}{2}\left(\frac{\partial w_0}{\partial r}\right)^2$$
$$\varepsilon_\theta = \frac{u_0}{r} + z\frac{\phi}{r} \quad (4)$$
$$\gamma_{rz} = \frac{dw_0}{dr} + \phi$$

Where, ∂_r and ∂_θ are the normal strains and γ_{rz} is the shear strain. In non-local elasticity theory, the effects of small scale and interatomic bonds come directly to the constitutive equations as material parameters [9]. Eringen presented a differential form of the non-local constitutive equation from non-local balance law as follows [12-13]:

$$\left(1-\mu\nabla^2\right)\sigma^{NL} = \sigma^L = C\varepsilon, \mu = \left(e_0 a\right)^2$$
$$C = \begin{bmatrix} \frac{E_1}{1-\upsilon_{12}\upsilon_{21}} & \frac{\upsilon_{12}E_2}{1-\upsilon_{12}\upsilon_{21}} & 0 \\ \frac{\upsilon_{12}E_2}{1-\upsilon_{12}\upsilon_{21}} & \frac{E_2}{1-\upsilon_{12}\upsilon_{21}} & 0 \\ 0 & 0 & kG_{23}h \end{bmatrix} \quad (5)$$

In which, a is internal characteristic length and e_0 is material constant which is defined by experiment. The parameter $e_0 a$ is the small-scale parameter and depends on boundary condition, chirality, mode shapes, number of walls and the nature of motions. Also, ∇^2 is the Laplacian operator which is defined by:

$$\nabla^2 = \frac{d^2}{dr^2} + \frac{1}{r}\frac{d}{dr} \quad (6)$$

The non-local force, moment and shear force components $N_r^{NL}, N_\theta^{NL}, M_r^{NL}, M_\theta^{NL}$ and Q_r^{NL} are introduced as follows:

$$\begin{Bmatrix} N_r \\ N_\theta \end{Bmatrix}^{NL} = \int_{-\frac{h}{2}}^{\frac{h}{2}} \begin{Bmatrix} \sigma_r \\ \sigma_\theta \end{Bmatrix}^{NL} dz$$
$$\begin{Bmatrix} M_r \\ M_\theta \end{Bmatrix}^{NL} = \int_{-\frac{h}{2}}^{\frac{h}{2}} \begin{Bmatrix} \sigma_r \\ \sigma_\theta \end{Bmatrix}^{NL} z dz \quad (7)$$
$$Q_r^{NL} = \int_{-\frac{h}{2}}^{\frac{h}{2}} \sigma_{rz}^{NL} dz$$

By substituting stress values into resultant forces, the following constitutive relations are obtained:

$$N_r^L = \left(Q_{11}\overset{0}{\varepsilon}_r + Q_{12}\overset{0}{\varepsilon}_\theta\right)h$$
$$N_\theta^L = \left(Q_{12}\overset{0}{\varepsilon}_r + Q_{22}\overset{0}{\varepsilon}_\theta\right)h$$
$$M_r^L = \left(Q_{11}\overset{1}{\varepsilon}_r + Q_{12}\overset{1}{\varepsilon}_\theta\right)\frac{h^3}{12} \quad (8)$$
$$M_\theta^L = \left(Q_{12}\overset{1}{\varepsilon}_r + Q_{22}\overset{1}{\varepsilon}_\theta\right)\frac{h^3}{12}$$
$$Q_r^L = C_{44}\overset{0}{\gamma}_{rz}\, h$$

By substituting strains and stiffness matrix in terms of displacements and material constant, respectively, the following relations are obtained:

$$N_r^L = \frac{E_1 h}{1-\upsilon_{12}\upsilon_{21}}\left(\frac{\partial u_0}{\partial r} + \frac{1}{2}\left(\frac{\partial w_0}{\partial r}\right)^2\right) + \frac{\upsilon_{12}E_2 h}{1-\upsilon_{12}\upsilon_{21}}\frac{u_0}{r}$$
$$N_\theta^L = \frac{\upsilon_{12}E_2 h}{1-\upsilon_{12}\upsilon_{21}}\left(\frac{\partial u_0}{\partial r} + \frac{1}{2}\left(\frac{\partial w_0}{\partial r}\right)^2\right) + \frac{E_2 h}{1-\upsilon_{12}\upsilon_{21}}\frac{u_0}{r} \quad (9)$$
$$M_r^L = \frac{E_1 h^3}{12\left(1-\upsilon_{12}\upsilon_{21}\right)}\frac{\partial\phi}{\partial r} + \frac{\upsilon_{12}E_2 h^3}{12\left(1-\upsilon_{12}\upsilon_{21}\right)}\frac{1}{r}\phi$$
$$M_\theta^L = \frac{\upsilon_{12}E_2 h^3}{12\left(1-\upsilon_{12}\upsilon_{21}\right)}\frac{\partial\phi}{\partial r} + \frac{E_2 h^3}{12\left(1-\upsilon_{12}\upsilon_{21}\right)}\frac{1}{r}\phi$$
$$Q_r^L = kG_{23}h\left(\frac{\partial w_0}{\partial r} + \phi\right)$$

Based on the principle of minimum total potential energy, the following variations can be obtained for a system in equilibrium state:

$$\delta\Pi = \delta U + \delta\Omega = 0$$
$$\delta\Omega = \iint_A N\frac{\partial}{\partial r}\left(\delta u_0\right) r dr d\theta \quad (10)$$
$$\delta U = \iiint_V \left(\sigma_r\delta\varepsilon_r + \sigma_\theta\delta\varepsilon_\theta + \sigma_{rz}\delta\gamma_{rz}\right)dV$$

Where, δ is the variation symbol. Also, U and Ω denote strain energy and potential of applied forces, respectively. By using the nonlocal stress resultants and energy relations, the non-local governing equations are defined as follows:

$$
\begin{aligned}
&1st: \frac{1}{r}N_r^{NL}+\frac{\partial N_r^{NL}}{\partial r}-\frac{1}{r}N_\theta^{NL}=0\\
&2nd: k_0\left(w_1-w_2\right)-N\nabla^2(w_1)\\
&+\frac{\partial Q_r^{NL}}{\partial r}+\frac{1}{r}Q_r^{NL}=0\\
&3th: \frac{\partial M_r^{NL}}{\partial r}+\frac{1}{r}M_r^{NL}-\frac{1}{r}M_\theta^{NL}-Q_r^{NL}=0
\end{aligned}
\tag{11}
$$

$$
\begin{aligned}
&4th: \frac{1}{r}N_r^{NL}+\frac{\partial N_r^{NL}}{\partial r}-\frac{1}{r}N_\theta^{NL}=0\\
&5th: k_0\left(w_2-w_1\right)-k_w w_2+k_p\nabla^2 w_2-\\
&N\nabla^2(w_2)+\frac{\partial Q_r^{NL}}{\partial r}+\frac{1}{r}Q_r^{NL}=0\\
&6th: \frac{\partial M_r^{NL}}{\partial r}+\frac{1}{r}M_r^{NL}-\frac{1}{r}M_\theta^{NL}-Q_r^{NL}=0
\end{aligned}
\tag{12}
$$

In which, "Eqs. (11)" are related to the upper layer and "Eqs. (12)" are corresponded to the lower layer. Also, k_w and k_p are the Winkler and Pasternak stiffness coefficient of the elastic foundation, respectively and k_0 is the linear van der Waals interaction coefficient. Using "Eqs. (9), (11) and (12)" yield the following relations:

$$
\begin{aligned}
&1st: \frac{1}{r}\left(\frac{E_1h}{1-\upsilon_{12}\upsilon_{21}}\left(\frac{\partial u_1}{\partial r}+\frac{1}{2}(\frac{\partial w_1}{\partial r})^2\right)+\frac{\upsilon_{12}E_2h}{1-\upsilon_{12}\upsilon_{21}}\frac{u_1}{r}\right)+\frac{E_1h}{1-\upsilon_{12}\upsilon_{21}}\left(\frac{\partial^2 u_1}{\partial r^2}+\frac{\partial w_1}{\partial r}\frac{\partial^2 w_1}{\partial r^2}\right)+\frac{\upsilon_{12}E_2h}{1-\upsilon_{12}\upsilon_{21}}\left(\frac{1}{r}\frac{\partial u_1}{\partial r}-\frac{u_1}{r^2}\right)\\
&-\frac{1}{r}\left(\frac{\upsilon_{12}E_2h}{1-\upsilon_{12}\upsilon_{21}}\left(\frac{\partial u_1}{\partial r}+\frac{1}{2}(\frac{\partial w_1}{\partial r})^2\right)-\frac{E_2h}{1-\upsilon_{12}\upsilon_{21}}\frac{u_1}{r}\right)=0\\
&2nd: \left(1-\mu\nabla^2\right)\left(k_0\left(w_1-w_2\right)-N\nabla^2(w_1)\right)+kG_{23}h\left(\frac{\partial^2 w_1}{\partial r^2}+\frac{\partial\phi_1}{\partial r}\right)+\frac{1}{r}kG_{23}h\left(\frac{\partial w_1}{\partial r}+\phi_1\right)=0\\
&3th: \frac{E_1h^3}{12\left(1-\upsilon_{12}\upsilon_{21}\right)}\frac{\partial^2\phi_1}{\partial r^2}+\frac{\upsilon_{12}E_2h^3}{12\left(1-\upsilon_{12}\upsilon_{21}\right)}\frac{1}{r}\left(\frac{\partial\phi_1}{\partial r}-\frac{\phi_1}{r}\right)+\frac{1}{r}\left(\frac{E_1h^3}{12\left(1-\upsilon_{12}\upsilon_{21}\right)}\frac{\partial\phi_1}{\partial r}+\frac{\upsilon_{12}E_2h^3}{12\left(1-\upsilon_{12}\upsilon_{21}\right)}\frac{\phi_1}{r}\right)\\
&-\frac{1}{r}\left(\frac{\upsilon_{12}E_2h^3}{12\left(1-\upsilon_{12}\upsilon_{21}\right)}\frac{\partial\phi_1}{\partial r}-\frac{E_2h^3}{12\left(1-\upsilon_{12}\upsilon_{21}\right)}\frac{\phi_1}{r}\right)-kG_{23}h\left(\frac{\partial w_1}{\partial r}+\phi_1\right)=0\\
&4th: \frac{1}{r}\left(\frac{E_1h}{1-\upsilon_{12}\upsilon_{21}}\left(\frac{\partial u_2}{\partial r}+\frac{1}{2}(\frac{\partial w_2}{\partial r})^2\right)+\frac{\upsilon_{12}E_2h}{1-\upsilon_{12}\upsilon_{21}}\frac{u_2}{r}\right)+\frac{E_1h}{1-\upsilon_{12}\upsilon_{21}}\left(\frac{\partial^2 u_2}{\partial r^2}+\frac{\partial w_2}{\partial r}\frac{\partial^2 w_2}{\partial r^2}\right)+\frac{\upsilon_{12}E_2h}{1-\upsilon_{12}\upsilon_{21}}\frac{1}{r}\left(\frac{\partial u_2}{\partial r}-\frac{u_2}{r}\right)\\
&-\frac{1}{r}\left(\frac{\upsilon_{12}E_2h}{1-\upsilon_{12}\upsilon_{21}}\left(\frac{\partial u_2}{\partial r}+\frac{1}{2}(\frac{\partial w_2}{\partial r})^2\right)-\frac{E_2h}{1-\upsilon_{12}\upsilon_{21}}\frac{u_2}{r}\right)=0\\
&5th: \left(1-\mu\nabla^2\right)\left(k_0\left(w_2-w_1\right)-k_w w_2+k_p\nabla^2 w_2-N\nabla^2(w_2)\right)+kG_{23}h\left(\frac{\partial^2 w_2}{\partial r^2}+\frac{\partial\phi_2}{\partial r}\right)+kG_{23}h\frac{1}{r}\left(\frac{\partial w_2}{\partial r}+\phi_2\right)=0\\
&6th: \frac{E_1h^3}{12\left(1-\upsilon_{12}\upsilon_{21}\right)}\frac{\partial^2\phi_2}{\partial r^2}+\frac{\upsilon_{12}E_2h^3}{12\left(1-\upsilon_{12}\upsilon_{21}\right)}\frac{1}{r}\left(\frac{\partial\phi_2}{\partial r}-\frac{\phi_2}{r}\right)+\frac{1}{r}\left(\frac{E_1h^3}{12\left(1-\upsilon_{12}\upsilon_{21}\right)}\frac{\partial\phi_2}{\partial r}+\frac{\upsilon_{12}E_2h^3}{12\left(1-\upsilon_{12}\upsilon_{21}\right)}\frac{\phi_2}{r}\right)\\
&-\frac{1}{r}\left(\frac{\upsilon_{12}E_2h^3}{12\left(1-\upsilon_{12}\upsilon_{21}\right)}\frac{\partial\phi_2}{\partial r}-\frac{E_2h^3}{12\left(1-\upsilon_{12}\upsilon_{21}\right)}\frac{\phi_2}{r}\right)-kG_{23}h\left(\frac{\partial w_2}{\partial r}+\phi_2\right)=0
\end{aligned}
\tag{13}
$$

Then, by substituting "Eq. (6)" in 2nd and 5th relations of "Eq. (13)", they are transformed as follows:

$$\begin{aligned}
&2.k_0(w_1-w_2)-N\left(\frac{\partial^2 w_1}{\partial r^2}+\frac{1}{r}\frac{\partial w_1}{\partial r}\right)-\\
&k_0\mu\left(\frac{\partial^2 w_1}{\partial r^2}+\frac{1}{r}\frac{\partial w_1}{\partial r}-\frac{\partial^2 w_2}{\partial r^2}-\frac{1}{r}\frac{\partial w_2}{\partial r}\right)\\
&+\mu N\left(\frac{\partial^4 w_1}{\partial r^4}+\frac{2}{r}\frac{\partial^3 w_1}{\partial r^3}+\frac{1}{r^2}\frac{\partial^2 w_1}{\partial r^2}+\frac{1}{r^3}\frac{\partial w_1}{\partial r}\right)\\
&+kG_{23}h\left(\frac{\partial^2 w_1}{\partial r^2}+\frac{\partial \phi_1}{\partial r}\right)+kG_{23}h\frac{1}{r}\left(\frac{\partial w_1}{\partial r}+\phi_1\right)=0
\end{aligned} \tag{14}$$

$$\begin{aligned}
&5.k_0\left(w_2-w_1\right)-k_w w_2+k_p\left(\frac{\partial^2 w_2}{\partial r^2}+\frac{1}{r}\frac{\partial w_2}{\partial r}\right)\\
&-N\left(\frac{\partial^2 w_2}{\partial r^2}+\frac{1}{r}\frac{\partial w_2}{\partial r}\right)\\
&-k_0\mu\left(\frac{\partial^2 w_2}{\partial r^2}-\frac{\partial^2 w_1}{\partial r^2}+\frac{1}{r}\frac{\partial w_2}{\partial r}-\frac{1}{r}\frac{\partial w_1}{\partial r}\right)\\
&+k_w\mu\left(\frac{\partial^2 w_2}{\partial r^2}+\frac{1}{r}\frac{\partial w_2}{\partial r}\right)\\
&-k_p\mu\left(\frac{\partial^4 w_2}{\partial r^4}+\frac{2}{r}\frac{\partial^3 w_2}{\partial r^3}-\frac{1}{r^2}\frac{\partial^2 w_2}{\partial r^2}+\frac{1}{r^3}\frac{\partial w_2}{\partial r}\right)\\
&+\mu N\left(\frac{\partial^4 w_2}{\partial r^4}+\frac{2}{r}\frac{\partial^3 w_2}{\partial r^3}+\frac{1}{r^2}\frac{\partial^2 w_2}{\partial r^2}+\frac{1}{r^3}\frac{\partial w_2}{\partial r}\right)\\
&+kG_{23}h\left(\frac{\partial^2 w_2}{\partial r^2}+\frac{\partial \phi_2}{\partial r}\right)\\
&+\frac{1}{r}kG_{23}h\left(\frac{\partial w_2}{\partial r}+\phi_2\right)=0
\end{aligned} \tag{15}$$

The following boundary conditions are defined for both inner and outter edges of annular plates based on FSDT as follows:

Simply supported boundary condition (S)

$$u=w=M_r=0 \tag{16}$$

Clamped boundary condition (C)

$$u=w=\phi=0 \tag{17}$$

3 SOLUTION

In this paper, in order to solve the equilibrium equations, the Differential Quadrature Method (DQM) has been employed. This method offers accuracy, efficiency, convenience and great potential in solving complicated partial differential equations [28]. Therefore, the DQ method, as well as simple formulation, provides low computational cost in contrast with other numerical methods such as Dynamic Relaxation (DR), Finite Difference (FD), Finite Element (FE), and etc. The Differential Quadrature (DQ) method was introduced by Bellman and Casti [46-47]. Recently, many researchers have extensively supported the application of the DQM for investigation of nanostructures [48–51]. The basic idea of the differential quadrature method is based on the approximation of partial derivative of a function with respect to a space variable at a discrete point as a weighted linear sum of the function values at all discrete points in the whole domain. Its weighting coefficients solely depend on the grid spacing. Therefore, every partial differential equation can be simplified to a number of algebraic equations using these coefficients [52]. DQM can be subdivided into several subsets with respect to the applied function and satisfied types of boundary conditions. In this paper, polynomial function and direct substitution technique are used for this goal. By using the DQM, derivatives of a function f_r at point r_i are defined as follows:

$$\left.\frac{d^{(n)}f}{dr}\right|_{r_i}=\sum_{k=1}^{M}A_{ik}^{(n)}f(r_i)\quad i=1,...,M \tag{18}$$

$A_{ik}^{(n)}$ is the respective weighting coefficient related to the nth-order derivative obtained as follows:

$$A_{ij}^{(n)}=n\left[A_{ij}^{1}A_{ii}^{(n-1)}-\frac{A_{ij}^{(n-1)}}{\left(r_i-r_j\right)}\right]\quad i\neq j \tag{19}$$

$$A_{ii}^{(n)}=-\sum_{j=1,\neq i}^{M}A_{ij}^{(n)}\quad i,j=1...M \tag{20}$$

In which, M is the number of grid points along r direction.

It is more offered to use the grid point distribution which is based on Gauss–Chebyshev–Lobatto points to gain more accurate results [32]. According to the Gauss–Chebyshev– Lobatto grid point's distribution, the coordinates of the grid points are as follows:

$$r_i=\left(\frac{r}{2}-\cos\left(\left(\frac{i-1}{M-1}\right)\pi\right)\left(\frac{r}{2}\right)\right),i=1,...,M \tag{21}$$

With implementation of DQM into the "Eq. (13)", the following buckling equations are obtained:

$$2nd: k_0\left(w_1^1 - w_2^1\right)$$
$$-N\left(\sum_{k=1}^{M} C_{ik}^2 w_{1kj}^1 + \frac{1}{r}\sum_{k=1}^{M} C_{ik} w_{1kj}^1\right)$$
$$-k_0\mu\left(\begin{array}{l}\sum_{k=1}^{M} C_{ik}^2 w_{1kj}^1 + \frac{1}{r}\sum_{k=1}^{M} C_{ik} w_{1kj}^1 \\ -\sum_{k=1}^{M} C_{ik}^2 w_{2kj}^1 - \frac{1}{r}\sum_{k=1}^{M} C_{ik} w_{2kj}^1\end{array}\right)$$
$$+\mu N\left(\begin{array}{l}\sum_{k=1}^{M} C_{ik}^4 w_{1kj}^1 \\ +\frac{2}{r}\sum_{k=1}^{M} C_{ik}^3 w_{1kj}^1 + \frac{1}{r^2}\sum_{k=1}^{M} C_{ik}^2 w_{1kj}^1 + \frac{1}{r^3}\sum_{k=1}^{M} C_{ik} w_{1kj}^1\end{array}\right)$$
$$+kG_{23}h\left(\sum_{k=1}^{M} C_{ik}^2 w_{1kj}^1 + \sum_{k=1}^{M} C_{ik}\phi_{1kj}^1\right)$$
$$+kG_{23}h\frac{1}{r}\left(\sum_{k=1}^{M} C_{ik} w_{1kj}^1 + \phi_1^1\right) = 0$$

$$3th: \frac{E_1 h^3}{12\left(1-\upsilon_{12}\upsilon_{21}\right)}\sum_{k=1}^{M} C_{ik}^2 \phi_{1kj}^1$$
$$+\frac{\upsilon_{12}E_2 h^3}{12\left(1-\upsilon_{12}\upsilon_{21}\right)}\frac{1}{r}\left(\sum_{k=1}^{M} C_{ik}\phi_{1kj}^1 - \frac{\phi_1^1}{r}\right)$$
$$+\frac{1}{r}\left(\frac{E_1 h^3}{12\left(1-\upsilon_{12}\upsilon_{21}\right)}\sum_{k=1}^{M} C_{ik}\phi_{1kj}^1 + \frac{\upsilon_{12}E_2 h^3}{12\left(1-\upsilon_{12}\upsilon_{21}\right)}\frac{\phi_1^1}{r}\right)$$
$$-\frac{1}{r}\left(\frac{\upsilon_{12}E_2 h^3}{12\left(1-\upsilon_{12}\upsilon_{21}\right)}\sum_{k=1}^{M} C_{ik}\phi_{1kj}^1 - \frac{E_2 h^3}{12\left(1-\upsilon_{12}\upsilon_{21}\right)}\frac{\phi_1^1}{r}\right)$$
$$-kG_{23}h\left(\sum_{k=1}^{M} C_{ik} w_{1kj}^1 + \phi_1^1\right) = 0$$

$$5th: k_0\left(w_2^1 - w_1^1\right) - k_w w_2^1$$
$$+k_p\left(\sum_{k=1}^{M} C_{ik}^2 w_{2kj}^1 + \frac{1}{r}\sum_{k=1}^{M} C_{ik} w_{2kj}^1\right)$$
$$-N\left(\sum_{k=1}^{M} C_{ik}^2 w_{2kj}^1 + \frac{1}{r}\sum_{k=1}^{M} C_{ik} w_{2kj}^1\right)$$
$$-k_0\mu\left(\begin{array}{l}\sum_{k=1}^{M} C_{ik}^2 w_{2kj}^1 \\ -\sum_{k=1}^{M} C_{ik}^2 w_{1kj}^1 + \frac{1}{r}\sum_{k=1}^{M} C_{ik} w_{2kj}^1 - \frac{1}{r}\sum_{k=1}^{M} C_{ik} w_{1kj}^1\end{array}\right)$$
$$+k_w\mu\left(\sum_{k=1}^{M} C_{ik}^2 w_{2kj}^1 + \frac{1}{r}\sum_{k=1}^{M} C_{ik} w_{2kj}^1\right)$$
$$-k_p\mu\left(\begin{array}{l}\sum_{k=1}^{M} C_{ik}^4 w_{2kj}^1 + \frac{2}{r}\sum_{k=1}^{M} C_{ik}^3 w_{2kj}^1 \\ -\frac{1}{r^2}\sum_{k=1}^{M} C_{ik}^2 w_{2kj}^1 + \frac{1}{r^3}\sum_{k=1}^{M} C_{ik} w_{2kj}^1\end{array}\right)$$
$$+\left(\mu N\left(\begin{array}{l}\sum_{k=1}^{M} C_{ik}^4 w_{2kj}^1 + \frac{2}{r}\sum_{k=1}^{M} C_{ik}^3 w_{2kj}^1 \\ +\frac{1}{r^2}\sum_{k=1}^{M} C_{ik}^2 w_{2kj}^1 + \frac{1}{r^3}\sum_{k=1}^{M} C_{ik} w_{2kj}^1\end{array}\right)\right)$$
$$+kG_{23}h\left(\sum_{k=1}^{M} C_{ik}^2 w_{2kj}^1 + \sum_{k=1}^{M} C_{ik}\phi_{2kj}^1\right)$$
$$+\frac{1}{r}kG_{23}h\left(\sum_{k=1}^{M} C_{ik} w_{2kj}^1 + \phi_2^1\right) = 0$$

(22)

$$6th: \frac{E_1 h^3}{12\left(1-\upsilon_{12}\upsilon_{21}\right)}\sum_{k=1}^{M} C_{ik}^2 \phi_{2kj}^1$$
$$+\frac{\upsilon_{12}E_2 h^3}{12\left(1-\upsilon_{12}\upsilon_{21}\right)}\frac{1}{r}\left(\sum_{k=1}^{M} C_{ik}\phi_{2kj}^1 - \frac{\phi_2^1}{r}\right)$$
$$+\frac{1}{r}\left(\begin{array}{l}\frac{E_1 h^3}{12\left(1-\upsilon_{12}\upsilon_{21}\right)}\sum_{k=1}^{M} C_{ik}\phi_{2kj}^1 \\ +\frac{\upsilon_{12}E_2 h^3}{12\left(1-\upsilon_{12}\upsilon_{21}\right)}\frac{\phi_2^1}{r}\end{array}\right)$$
$$-\frac{1}{r}\left(\begin{array}{l}\frac{\upsilon_{12}E_2 h^3}{12\left(1-\upsilon_{12}\upsilon_{21}\right)}\sum_{k=1}^{M} C_{ik}\phi_{2kj}^1 \\ -\frac{E_2 h^3}{12\left(1-\upsilon_{12}\upsilon_{21}\right)}\frac{\phi_2^1}{r}\end{array}\right)$$
$$-kG_{23}h\left(\sum_{k=1}^{M} C_{ik} w_{2kj}^1 + \phi_2^1\right) = 0$$

(23)

4 RESULT AND DISCUSSION

In this paper, mechanical buckling behavior of the orthotropic nanoplate embedded in an elastic matrix is investigated based on nonlocal FSDT and von Karman nonlinear strains. As mentioned, the elastic matrix is modeled as a Pasternak two parameters elastic foundation. In the parametric study, unless stated otherwise, the following foundation coefficients, material properties and dimensions are used for the nanoplate [38], [51]:

$$\begin{aligned} &E_1 = 1765\ (GPa)\\ &E_2 = 1584\ (GPa)\\ &\nu_{12} = 0.3\\ &\nu_{21} = 0.25\\ &h = 0.335\ (nm)\\ &k_w = 2\ (GPa/nm)\\ &k_p = 2\ (Pa.m)\\ &k_o = 45\ (GPa/m)\\ &e_0a = 1\ (nm)\\ &r_i = 1\ (nm)\\ &r_o = 5\ (nm) \end{aligned} \tag{24}$$

In this section, some comparison studies have been presented for verifying the results and formulations firstly and then the effects of different parameters are considered on the mechanical buckling of circular and annular bi-layered nanoplate.

4.1. Comparison Study

In this part, the current results are compared with those of [56] for non-dimensional linear buckling load of isotropic circular nanoplate with clamped boundary conditions which is defined in "Eq. (25)".

$$\varepsilon_b = \frac{14.6819h^2}{12\left(r^2 + 14.6819\left(e_0a\right)^2\right)\left(1-\nu^2\right)} \tag{25}$$

In which, ∂_b is the critical buckling load. As seen in "Table 1", the buckling load is presented for different values of nonlocal parameters and radiuses with $h = 0.335nm\ , \nu = 0.3$. As indicated, the results of present work are in good agreement with those of [56]. However, a minor difference between the current results and those obtained by [56] is due to the existing differences of defined boundary conditions in each work, solution methodology and also type of plate theory (used FSDT and CPT).

Table 1 Comparison of critical buckling load of isotropic annular/circular bilayer graphene sheet obtained by the present study (FSDT) with those of [56] (CPT) of clamped boundary condition.

	ε_b (%)				
	Small scale effect (nm)				
Radius (nm)	0	0.5	1	1.5	2
4	0.9205	0.7487	0.4800	0.3003	0.1986
4[56]	0.9430	0.7671	0.4918	0.3077	0.2019
6	0.4146	0.3763	0.2945	0.2162	0.1576
6[56]	0.4191	0.3803	0.2977	0.2186	0.1593
8	0.2343	0.2216	0.1906	0.1546	0.1222
8[56]	0.2358	0.2230	0.1918	0.1555	0.1229
10	0.1503	0.1450	0.1311	0.1130	0.0947
10[56]	0.1509	0.1455	0.1316	0.1134	0.0951

4.2. Parametric Study

In this section, several parametric studies are presented to reveal the effects of nonlocal parameter, radius, van der Waals variation, elastic foundation and boundary condition on the buckling load response of orthotropic bilayer graphene sheet based on nonlocal continuum mechanics. In order to show the importance of nonlocal parameter, "Fig. 2" shows the effect of nonlocal parameter on the buckling load in terms of radius of nanoplate for (a) clamped and (b) simply-supported boundary conditions. As seen, with increase of small scale parameter, the buckling load decreases. Also, with raising the radius of nanoplate the slope of curves reduces.

As indicated the buckling load of simply supported cases is lower than those of clamped ones in different values of small scale parameters. It is obvious that with increase of nanoplate radius from 5 to 20 nm, the slope of curves reduces and by increasing the radius from 20 nm the slope increases. In radius of 5 nm and small scale effect of 2 nm, the difference between the results obtained with local and nonlocal cases has the greatest value and this difference decreases by raising the radius from 5 to 20 nm. Also, by increase of small scale effect from 1 nm, the buckling load decreases first and then increases, but in small scale effect of 1.5 and 2 nm, with increase of radius, the buckling load increases continuously with smooth slope.

Unlike the simply supported boundary condition, in clamped case with increase of radius the difference between the local and nonlocal results decreases. Also, by increasing nanoplate radius, the difference of buckling load is higher in simply supported boundary condition compared to clamp one.

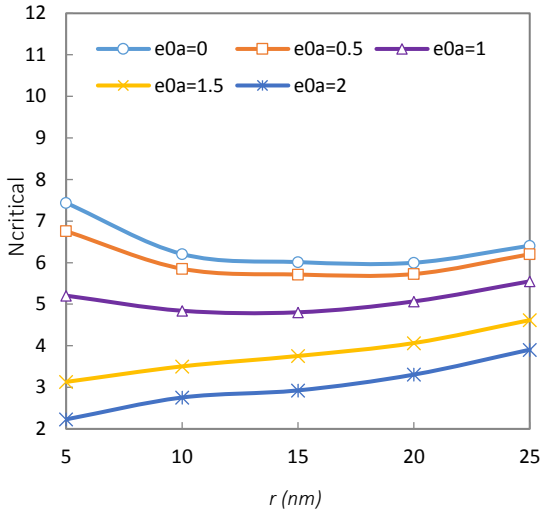

(a)

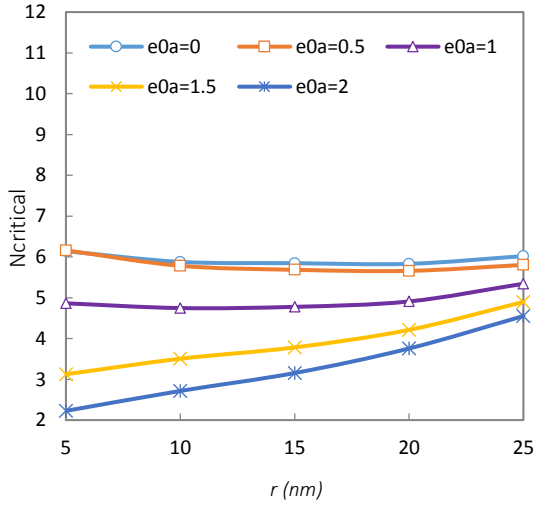

(b)

Fig. 2 Critical buckling load based on radius for: (a): clamped and (b): simply supported boundary conditions with various small scale parameters.

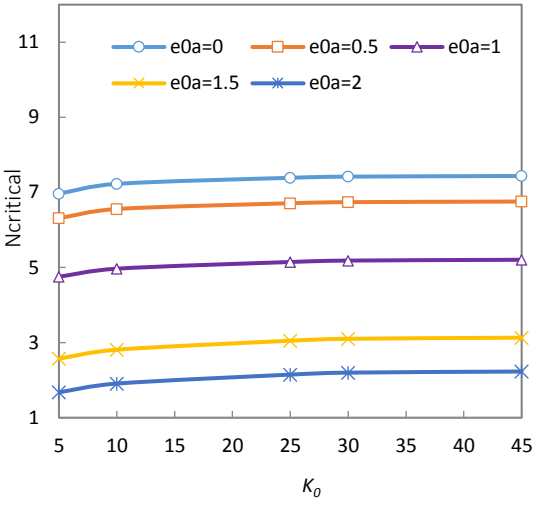

(a)

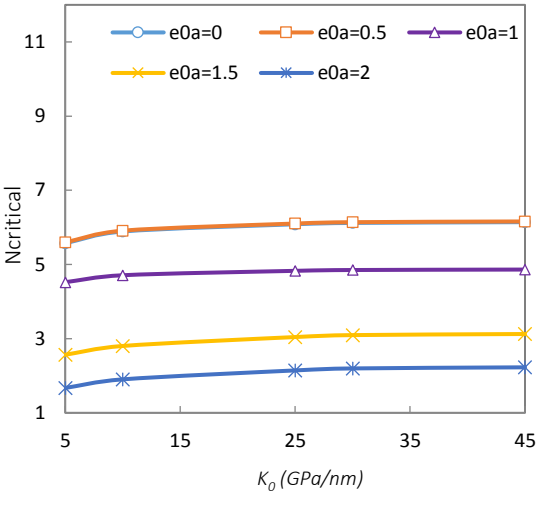

(b)

Fig. 3 Effect of vdW interaction coefficient on the critical buckling load for: (a): clamped and (b): simply supported boundary conditions with various nonlocal parameters.

In "Fig. 3" the effect of van der Waals variation on the buckling load has been studied for different small scale parameters with (a) clamped and (b) simply supported boundary conditions. It can be concluded that in clamped boundary condition, the difference between local and nonlocal models is larger than the simply supported one and as seen, unlike calmped boundary condition, in e_0a=0.5 nm there is no difference between local and nonlocal results in simply supported boundary condition. Also, as indicated, increase of vdW coefficient leads to increase of critical buckling load smoothly. The trend continues to the point that slope of the curves approximates to zero after a certain value in both boundary conditions and it can be seen that increase of vdW coefficient has no impact on critical buckling load after this value.

Figure 4 shows the effect of vdW interaction coefficient on the critical buckling load for different radiuses with (a) clamped and (b) simply-supported boundary conditions. From these figures increasing radius leads to increase of critical buckling load. Also, it is observed that with increasing vdW interaction coefficient the difference between the results obtained in nanoplate radius from 5 to 20 nm is smaller than this difference in radius from 25 nm up to the end. By comparing Figures a and b it can be concluded that this event is more noticeable in simply supported boundary condition case compared to clamped one.

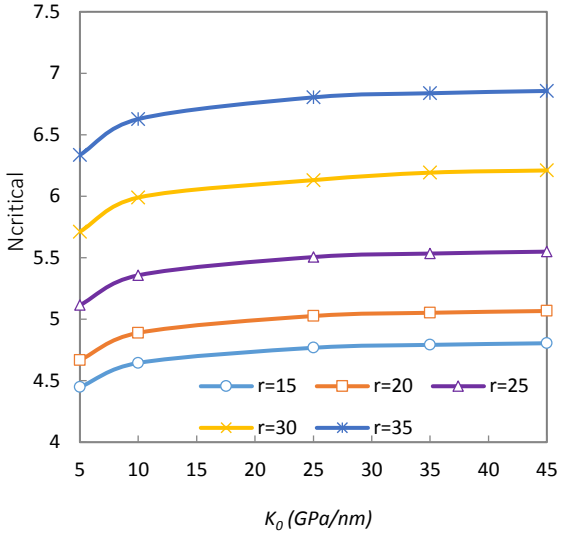

(a)

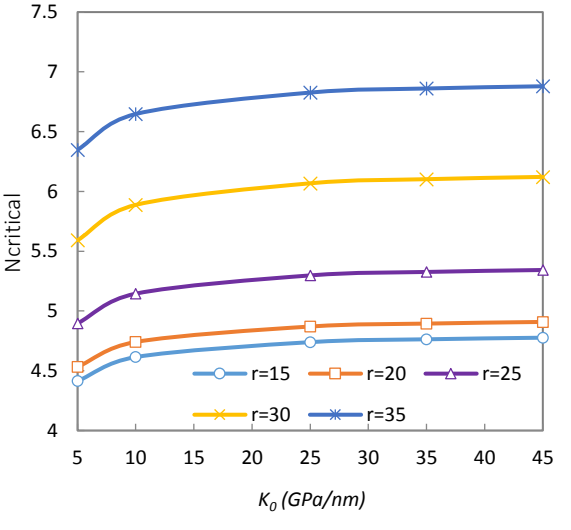

(b)

Fig. 4 Effect of vdW interaction coefficient on the critical buckling load for different radiuses in: (a): clamped and (b): simply supported boundary conditions.

In "Fig. 5", the effect of Winkler module on the buckling load is considered in different values of small scale parameter for (a) simply supported and (b) clamped boundary conditions. As it witnesses, by increasing the Winkler elastic foundation buckling load rises for both local and nonlocal models, but this behavior is more considerable in local state compared to nonlocal one for both types of boundary conditions. Also, by increase of small scale parameter the slope of curves leads to decrease. Furthermore, the difference between the results obtained with local and nonlocal cases is much greater in clamped compared to simply supported boundary condition and this trend is more significant with increase of Winkler module. As seen the small scale parameter does not have any effect on critical buckling load of the cases without elastic medium in simply supported boundary condition. However, unlike the clamped boundary condition, in simply supported case the influence of small scale parameter up to e_0a=1 nm remains almost constant on the results in the Winkler elastic foundation of 1 GPa per nanometer.

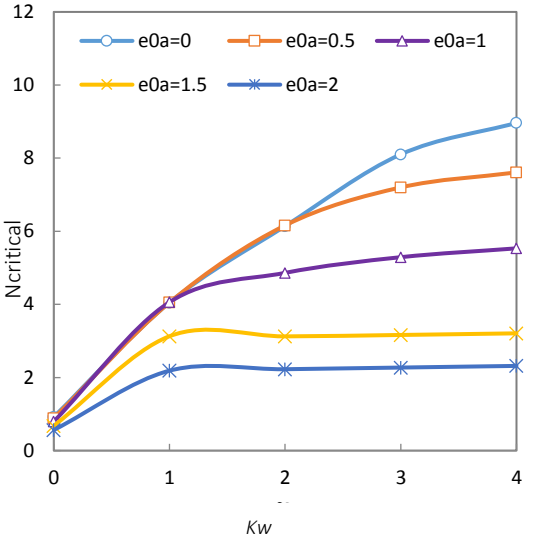

(a)

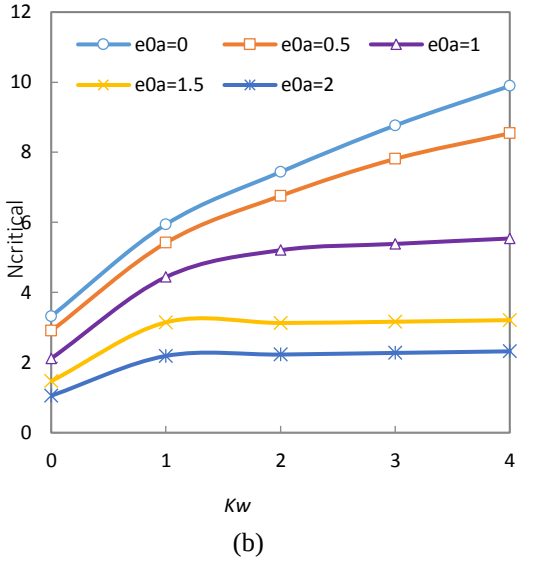

(b)

Fig. 5 Effect of Kw on critical buckling load for various small scale parameter with: (a): simply supported and (b): clamped boundary conditions.

Figure 6 shows the effect of shear module (Kp) of the elastic foundation on critical buckling load and two cases of nonlocal and local models with (a) simply supported and (b) clamped boundary conditions. As it is seen, increase in Kp leads to increase in critical buckling

load. In addition, from "Fig. 5", it can be found that the slope of the curves is wider in $0 < k_p < 0.5$ pa.m rather than the other value of Kp and therefore the effect of Kp is more significant in this range. Also, as seen, unlike the calmped boundary condition in simply supported case with increase of Kp there is no difference between the results obtained from local and nonlocal models with small scale parameter of 0.5 nm.

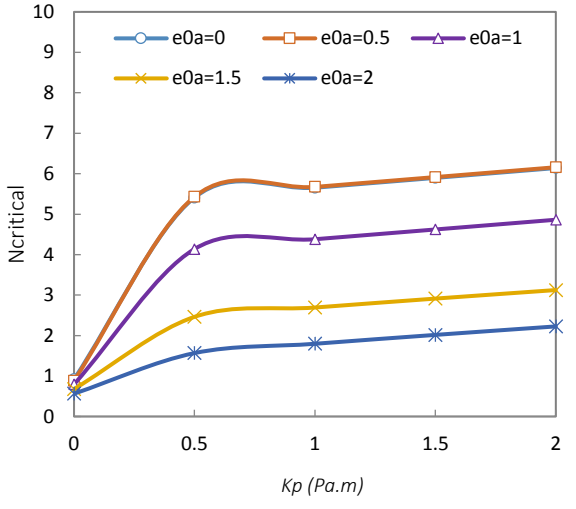

(a)

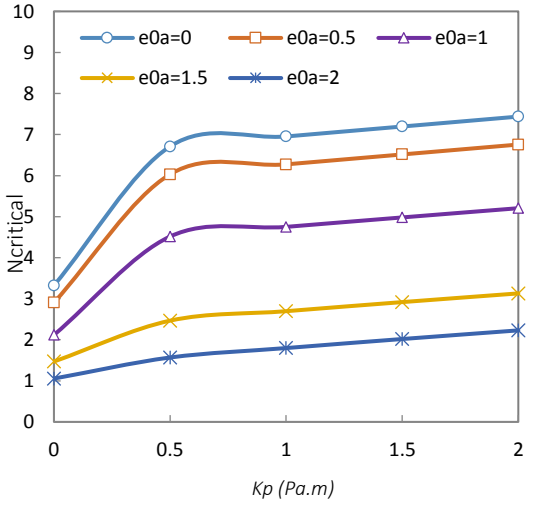

(b)

Fig. 6 Effect of Kp on critical buckling load for various small scale parameters with: (a): simply supported and (b): clamped boundary conditions.

5 CONCLUSION

In this paper, the mechanical buckling analysis of circular bilayer graphene sheet embedded in an elastic matrix is investigated based on nonlocal elasticity theory. Using the principle of virtual work, the nonlinear equilibrium equations are obtained in terms of the generalized displacements based on first order shear deformation theory using the nonlocal differential constitutive relations of Eringen and the von Karman nonlinear strains. Differential quadrature method is used to solve the governing equations for simply supported and clamped boundary conditions. To verify the present results and formulations, some comparison studies are carried out between the obtained results and the available solutions in the literature. From the results of present study following conclusions are noticeable:

- With increase of small scale parameter, the buckling load decreases. The slope of this reduction reduces with raising the radius of nanoplate.
- The critical buckling load of simply supported cases are lower those of clamped ones in different values of small scale parameters.
- The difference of buckling load between results obtained with local and nonlocal cases in radius of 5 nm and small scale effect of 2 nm has the greatest value and this difference decreases by raising the radius from 5 to 20 nm.
- Increase of vdW coefficient leads to increase of critical buckling load smoothly then it has no impact on critical buckling load after a certain value. After this value slope of the curves approximates to zero
- By increasing the Winkler elastic foundation, buckling load rises for both local and nonlocal models. This trend is more significant in local state compared to nonlocal one
- Small scale parameter does not have any effect on critical buckling load of cases without elastic medium in simply supported boundary condition.
- Increase in K_p leads to increase in critical buckling load. This trend is more considerable in the lower values of shear module.
- With increase of K_p there is no difference between the results obtained from local and nonlocal models with small scale parameter of 0.5 nanometer in simply supported boundary condition.

REFERENCES

[1] Sakhaee-Pour, A., Ahmadian, M. T., and Vafai, A., Applications of Single-Layered Graphene Sheets as Mass Sensors and Atomistic Dust Detectors, Solid State Commun, Vol. 145, 2008, pp. 168–172.

[2] Wang, J., Li, Z., Fan, G., Pan, H., Chen, Z., and Zhang, D., Reinforcement with Graphene Nano-Sheets in Aluminum Matrix Composites, Scr. Mater, Vol. 66, 2012, pp. 594–597.

[3] Drexler, K. E., Nanosystems: Molecular Machinery, Manufacturing and Computation, John Wiley & Sons Inc., 1992.

[4] Craighead, H. G., Nano Electro Mechanical Systems, Science, Vol. 290, 2000, pp. 1532–1535.

[5] Li, X., Bhushan, B., Takashima, K., Baek, C. W., and Kim, Y. K., Mechanical Characterization of Micro/Nanoscale Structures for MEMS/NEMS Applications Using Nanoindentation Techniques, Ultramicroscopy, Vol. 97, 2003, pp. 481–494.

[6] Pouresmaeeli, S., Fazelzadeh, S. A., and Ghavanloo, E., Exact Solution for Nonlocal Vibration of Double-Orthotropic Nanoplates Embedded in Elastic Medium, Composites Part B, Vol. 43, No. 8, 2012, pp. 3384–3390.

[7] Farajpour, A., ArabSolghar, A. R., and Shahidi, A. R., Postbuckling Analysis of Multilayered Graphene Sheets Under Non-Uniform Biaxial Compression, Physica E, Vol. 47, 2013, pp.197–206.

[8] Zhou, S. J., Li, Z. Q., Length Scales in The Static, Dynamic Torsion of a Circular Cylindrical Micro-Bar, J. Shanghai Univ. Technol., Vol. 31, 2001, pp. 401–407.

[9] Fleck, N. A., Hutchinson, J. W., Strain Gradient Plasticity, Adv. Appl. Mech., Vol. 33, 1997, pp. 296–358.

[10] Akgoz, B., Civalek, O., A Size-Dependent Shear Deformation Beam Model Based on the Strain Gradient Elasticity Theory, Internat. J. Engrg. Sci., Vol. 70, 2013, pp. 1–14.

[11] Malikan, M., Nguyen, V. B., Buckling Analysis of Piezo-Magnetoelectric Nanoplates in Hygrothermal Environment Based On a Novel One Variable Plate Theory Combining with Higher-Order Nonlocal Strain Gradient Theory, Physica E: Low-Dimensional System and Nanostructures, Vol. 102, 2018, pp. 8-28.

[12] Akgoz B., Civalek O., Free vibration analysis of axially functionally graded tapered Bernoulli–Euler microbeams based on the modified couple stress theory, Compos. Struct., Vol. 98, 2013, pp. 314–322.

[13] Yang F., Chong A.C.M., Lam D.C.C., Tong P., Couple stress based strain gradient theory for elasticity, Int. J. Solids Struct., Vol. 39, 2002, pp. 2731–2743.

[14] Malikan, M., Elctro-Mechanical Shear Buckling of Piezoelectric Nanoplate Using Modified Couple Stress Theory Based On Simplified First Order Shear Deformation Theory, Aplied Mathematical Modeling, Vol. 48, 2017, pp. 196-207.

[15] Eringen, A. C., Edelen, D. G. B., On Nonlocal Elasticity, Internat. J. Engrg. Sci., Vol. 10, 1972, pp. 233–248.

[16] Eringen, A. C., Nonlocal Continuum Field Theories, Springer, New York, 2002.

[17] Eringen, A. C., Nonlocal Continuum Mechanics Based on Distributions, Internat. J. Engrg. Sci., Vol. 44, 2006, pp. 141–147.

[18] Malikan, M., Dimitri, R., and Tornabene, F., Transient Response of Oscillated Carbon Nanotubes with an Internal and External Damping, Composites Part B: Engineering, Vol. 158, 2019, pp. 198-205.

[19] Reddy, J. N., Nonlocal Theories for Bending, Buckling and Vibration of Beams, Internat. J. Engrg. Sci., Vol. 45, 2007, pp. 288–307.

[20] Reddy, J. N., Pang, S. D., Nonlocal Continuum Theories of Beams for The Analysis of Carbon Nanotubes, J. Appl. Phys., Vol. 103, 2008, 023511.

[21] Murmu, T., Pradhan, S. C., Buckling Analysis of a Single-Walled Carbon Nanotube Embedded in an Elastic Medium Based On Nonlocal Elasticity and Timoshenko Beam Theory and Using DQM, Physica E, Vol. 41, 2009, pp. 1232–1239.

[22] Murmu, T., Pradhan, S. C., Thermo-Mechanical Vibration of a Single-Walled Carbon Nanotube Embedded in an Elastic Medium Based On Nonlocal Elasticity Theory, Comput. Mater. Sci., Vol. 46, 2009, pp. 854–859.

[23] Wang, C. M., Duan, W. H., Free Vibration of Nanorings/Arches Based On Nonlocal Elasticity, J. Appl. Phys., Vol. 104, 2008, 014303.

[24] Demir, C., Civalek, O., Torsional and Longitudinal Frequency and Wave Response of Microtubules Based On the Nonlocal Continuum and Nonlocal Discrete Models, Appl. Math. Model, Vol. 37, No. 22, 2013, pp. 9355–9367.

[25] Civalek, O., Demir, C., and Akgoz, B., Static Analysis of Single Walled Carbon Nanotubes (SWCNT) Based on Eringen's Nonlocal Elasticity Theory, Int. J. Eng. Appl. Sci., Vol. 2, 2009, pp. 47–56.

[26] Zenkour, A. M., Nonlocal Transient Thermal Analysis of a Single-Layered Graphene Sheet Embedded in Viscoelastic Medium, Physica E, Vol. 97, 2016, pp. 87–97.

[27] Shen, H., Zhang, C. L., Torsional Buckling and Postbuckling of Double-Walled Carbon Nanotubes by Nonlocal Shear Deformable Shell Model, Compos. Struct., Vol. 92, 2010, pp. 1073–1084.

[28] Poot, M., van der Zant, H. S. J., Nanomechanical Properties of Few-Layer Graphene Membranes, Appl. Phys. Lett., Vol. 92, 2008, 063111.

[29] Pradhan, S. C., Phadikar, J. K., Small Scale Effect On Vibration of Embedded Multilayered Graphene Sheets Based On Nonlocal Continuum Models, Phys. Lett. A, Vol. 373, 2009, pp. 1062–1069.

[30] Pradhan, S. C., Buckling of Single Layer Graphene Sheet Based On Nonlocal Elasticity and Higher Order Shear Deformation Theory, Phys. Lett. A, Vol. 373, No. 45, 2009, pp. 4182–4188.

[31] Reddy, C. D., Rajendran, S., and Liew, K. M., Equilibrium Configuration and Continuum Elastic Properties of Finite Sized Graphene, Nanotechnology, Vol. 17, 2006, pp. 864–870.

[32] Shokrieh, M. M., Rafiee, R., Prediction of Young's Modulus of Graphene Sheets and Carbon Nanotubes Using Nanoscale Continuum Mechanics Approach, Mater. Des., Vol. 31, 2010, pp. 790–795.

[33] Sakhaee-Pour, A., Elastic Buckling of Single-Layered Graphene Sheet, Comput. Mater. Sci., Vol. 45, No. 2, 2009, pp. 266–270.

[34] Ansari, R., Rajabiehfard, R., and Arash, B., Nonlocal Finite Element Model for Vibrations of Embedded Multi Layered Graphene Sheets, Comput. Mater. Sci., Vol. 49, 2010, pp.831–838.

[35] Jomehzadeh, E., Saidi, A. R., A Study On Large Amplitude Vibration of Multilayered Graphene Sheets, Comput. Mater. Sci., Vol. 50, 2011, pp. 1043–1051.

[36] Aksencer, T., Aydogdu, M., Levy Type Solution Method for Vibration and Buckling of Nanoplates Using Nonlocal Elasticity Theory, Physica E, Vol. 43, 2011, pp. 954–959.

[37] Ghasemi, A., Dardel, M., Ghasemi, M. H., and Barzegari, M. M., Analytical Analysis of Buckling and Postbuckling of Fluid Conveying Multi-Walled Carbon Nanotubes, Appl. Math. Model, Vol. 37, 2013, pp. 4972–4992.

[38] Farajpour, A, Danesh, M, and Mohammadi, M. Buckling Analysis of Variable Thickness Nanoplates Using Nonlocal Continuum Mechanics, Physica E., Vol. 44, 2011, pp. 719–727.

[39] Pradhan, S. C., Murmu, T., Thermo-Mechanical Vibration of fgm Sandwich Beam Under Variable Elastic Foundations Using Differential Quadrature Method, J. Sound Vib., Vol. 321, 2009, pp. 342–362.

[40] Pradhan, S. C., Kumar, A., Vibration Analysis of Orthotropic Graphene Sheets Embedded in Pasternak Elastic Medium Using Nonlocal Elasticity Theory and Differential Quadrature Method, Comput. Mater. Sci., Vol. 50, 2010, pp. 239–245.

[41] Civalek, O., Akgoz, B., Vibration Analysis of Micro-Scaled Sector Shaped Graphene Surrounded by an Elastic Matrix, Comput. Mater. Sci., Vol. 77, 2013, pp. 295–303.

[42] Tsiatas, G. C., Yiotis, A. J., Size Effect On the Static, Dynamic and Buckling Analysis of Orthotropic Kirchhoff-Type Skew Micro-Plates Based On a Modified Couple Stress Theory: Comparison with The Nonlocal Elasticity Theory, Acta Mech., Vol. 226, 2015, pp. 1267–1281.

[43] Civalek, O., Elastic Buckling Behavior of Skew Shaped Single-Layer Graphene Sheets, Thin Solid Films, Vol. 550, 2013, pp. 450–458.

[44] Zenkour, A. M., Sobhy, M., Nonlocal Elasticity Theory for Thermal Buckling of Nanoplates Lying On Winkler–Pasternak Elastic Substrate Medium, Physica E, Vol. 53, 2013, pp. 251–259.

[45] Ansari, R., Sahmani, S., Prediction of Biaxial Buckling Behavior of Single-Layered Graphene Sheets Based On Nonlocal Plate Models and Molecular Dynamics Simulations, Applied Mathematical Modelling, Vol. 37, 2013, pp. 7338–7351.

[46] Farajpour, A., Dehghany, M., and Shahidi, A. R., Surface and Nonlocal Effects On the Axisymmetric Buckling of Circular Graphene Sheets in Thermal Environment, Composites: Part B, Vol. 50, 2013, pp. 333–343.

[47] Radebe, I. S., Adali, S., Buckling and Sensitivity Analysis of Nonlocal Orthotropic Nanoplates with Uncertain Material Properties, Composites: Part B, Vol. 56, 2014, pp. 840–846.

[48] Ansari, R., Shahabodini, A., Shojai, M. F., Mohammadi, V., and Gholami, R., On the Bending and Buckling Behaviors of Mindlin Nanoplates Considering Surface Energies, Physica E, Vol. 57, 2014, pp. 126–137.

[49] Anjomshoa, A., Shahidi, A. R., Hassani, B., and Jomehzadeh, E., Finite Element Buckling Analysis of Multi-Layered Graphene Sheets on Elastic Substrate Based on Nonlocal Elasticity Theory, Applied Mathematical Modelling, Vol. 38, No. 24, 2014, pp. 5934–5955.

[50] Mohammadi, M., Farajpou,r A., Moradi, A., and Ghayour, M., Shear Buckling of Orthotropic Rectangular Graphene Sheet Embedded in an Elastic Medium in Thermal Environment, Composites Part B, Vol. 56, 2014, pp. 629–637.

[51] Radic, N., Jeremic, D., Trifkovic, S., and Milutinovic, M., Buckling Analysis of Double-Orthotropic Nanoplates Embedded in Pasternak Elastic Medium Using Nonlocal Elasticity Theory, Composites: Part B, Vol. 61, 2014, pp. 162–171.

[52] Sarrami-Foroushani, S., Azhari, M., On the use of Bubble Complex Finite Strip Method in the Nonlocal Buckling and Vibration Analysis of Single-Layered Graphene Sheets, International Journal of Mechanical Sciences, Vol. 85, 2014, pp. 168-178.

[53] Sarrami-Foroushani, S., Azhari, M., Nonlocal Vibration and Buckling Analysis of Single and Multi-Layered Graphene Sheets Using Finite Strip Method Including Van Der Waals Effects, Physica E: Low-dimensional Systems and Nanostructures, Vol. 57, 2014, pp. 83-95.

[54] Murmu, T., Sienz, J., Adhikari, S., and Arnold, C., Nonlocal Buckling of Double-Nanoplate-Systems Under Biaxial Compression, Composites: Part B, Vol. 44, 2013, pp. 84–94.

[55] Farajpour, A., Shahidi, A. R., Mohammadi, M., and Mahzoon, M., Buckling of Orthotropic Micro/Nanoscale Plates Under Linearly Varying in-Plane Load Via Nonlocal Continuum Mechanics, Composite Structures, Vol. 94, 2012, pp. 1605–1615.

[56] Farajpour, A., Mohammadi, M., Shahidi, A. R., and Mahzoon, M., Axisymmetric Buckling of the Circular Graphene Sheets with the Nonlocal Continuum Plate Model, Physica E, Vol. 43, 2011, pp. 1820–1825.